

## Magnetic and Electrical Properties of $R_2\text{Mo}_2\text{O}_7$ Pyrochlore Compounds

NAUSHAD ALI, M. P. HILL, AND SUNIL LABROO

*Department of Physics and Molecular Science Program, Southern Illinois University, Carbondale, Illinois 62901*

AND J. E. GREEDAN

*Institute for Materials Research, McMaster University, Hamilton, Ontario, Canada L8S 4M1*

Received May 15, 1989; in revised form August 1, 1989

A combination of ac susceptibility, dc magnetization in a variety of applied fields, and electrical resistivity data is reported for five members of the  $R_2\text{Mo}_2\text{O}_7$  series of cubic pyrochlore structure oxides,  $R = \text{Nd, Sm, Gd, Tb, and Y}$ . These measurements extend published studies on the compounds and aid in the clarification and interpretation of the magnetic and electrical transport properties. The metallic ferromagnetics,  $R = \text{Nd, Sm, and Gd}$ , order at 96, 80, and 57 K, respectively. For  $R = \text{Nd}$  and  $\text{Sm}$  this is due most likely to ordering of Mo(IV) moments of about  $1 \mu_B$ . Near 30 K both compounds show hysteresis in the dc magnetization due to complex  $R$ -Mo coupling which give rise to resistivity minimum. For  $\text{Gd}_2\text{Mo}_2\text{O}_7$ , there is no low temperature hysteresis, indicating that both sublattices order ferromagnetically at the same temperature. A magnetization anomaly in semiconducting  $\text{Tb}_2\text{Mo}_2\text{O}_7$  at 25 K which is attributed to long range or short range magnetic order is reported for the first time and ac susceptibility data confirm a spin-glass like transition in  $\text{Y}_2\text{Mo}_2\text{O}_7$  reported previously. A correlation between the cubic lattice constant and the electrical and magnetic properties is noted. © 1989 Academic Press, Inc.

### 1. Introduction

Extensive studies of the pyrochlore compounds having the formula  $A_2B_2O_7$  (where  $A =$  a rare earth ion,  $B = \text{Ti}^{4+}, \text{V}^{4+},$  and  $\text{Mo}^{4+}$ ) have been performed (1). A series of rare earth molybdates  $R_2\text{Mo}_2\text{O}_7$  (where  $R = \text{Sm}$  and  $\text{Tb}$ ) has been prepared by Subramanian *et al.* (2). They reported the lattice constants and electrical properties and observed a semiconducting behavior in these compounds with an energy gap of a few millielectron volts. The magnetic properties were studied by Ranganathan *et al.* (3) in

the temperature range of from 77 to 300 K. They observed magnetic ordering temperature around or below 77 K. From their magnetic susceptibility data it is not possible to determine the magnetic ordering temperatures precisely.

More recently, rare earth molybdenum(IV) oxides with the composition  $R_2\text{Mo}_2\text{O}_7$  ( $R =$  rare earth) and the cubic pyrochlore structure have been studied recently with respect to crystallographic, magnetic, and electrical properties (4-7). These compounds show transitions from metallic to semiconducting behavior and

also complex magnetic properties as a function of  $R$ . For example, when  $R = \text{Nd, Sm, and Gd}$ , the compounds are metallic and ferromagnetic. Those with  $R = \text{Tb, Dy, Ho, Er, Tm, and Yb}$  are semiconducting. The latter three compounds with  $R = \text{Er, Tm, and Yb}$  appear to be simple paramagnets above 4.2 K. The phases with  $R = \text{Tb, Dy, and Ho}$  show evidence of remnant magnetic moments upon demagnetization at 4.2 K but no sign of a transition to a long range ordered state. Deviations from the Curie-Weiss law were observed for these compounds at temperatures near 20 K. A correlation between the cubic lattice constants and the electrical and magnetic properties is shown in Fig. 1. The metallic ferromagnets show a different linear dependence of lattice constant versus rare earth radius than those of the semiconducting phases.

For the ferromagnetic compounds  $R = \text{Nd, Sm, Gd}$  there were some discrepancies between the Curie temperatures determined by magnetization measurements rel-

ative to those determined from resistivity measurements. Magnetization versus temperature data for  $R = \text{Nd, Sm, and Gd}$  seemed to indicate  $T_c = 97, 93, \text{ and } 83 \text{ K}$ , respectively. The resistivity data, analyzed in terms of the temperature derivative, show lower  $T_c$ 's at 94 K (Nd) and 86 K (Sm) while two anomalies were found for Gd at 83 and 62 K. In addition, resistivity minima were observed in the 20 to 30 K range which correlated roughly with magnetization anomalies, but this relationship was not investigated in detail.

$\text{Y}_2\text{Mo}_2\text{O}_7$  for which only the molybdenum atoms are magnetic exhibits dc susceptibility behavior similar to that observed for spin glasses yet this material is crystalline and well ordered on the atomic scale (6).

In view of the remarkable properties of this series of compounds and the discrepancies noted above, further studies were carried out including ac susceptibility measurements which are very sensitive to magnetic ordering and dc magnetization

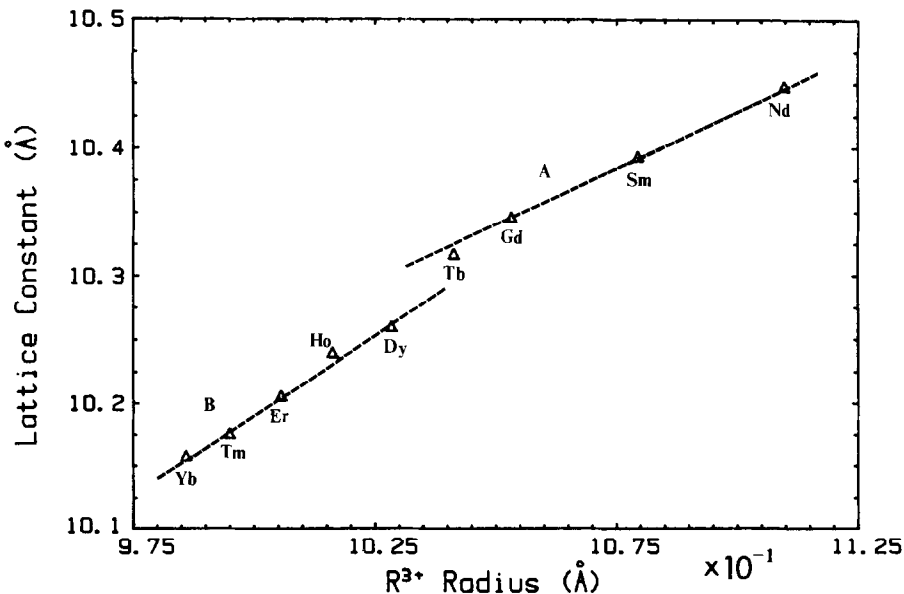


FIG. 1. Lattice constants for  $R_2\text{Mo}_2\text{O}_7$  (taken from Ref. (1)) as a function of  $R^{3+}$  radius for eightfold coordination (5).

measurements at very low (to  $1 \times 10^{-4}$  T) and at high applied fields (to 5.5 T). In all cases the samples were the same as those in Refs. (4, 5). Resistivity measurements were repeated to ensure that the sample behavior had not changed and to correlate with the ac susceptibility and dc magnetization data.

## 2. Experimental

The sample preparation, analysis, and characterization along with the lattice constants can be found in the work of Sato *et al.* (4). The starting materials were reagent grade  $R_2O_3$  powder (99.99%),  $MoO_3$  powder, and Mo metal powder (both 99.9%).  $MoO_2$  was prepared by heating a mixture of the appropriate molar ratio of  $MoO_3$  and Mo in vacuo at 700°C for 3 days. The general procedure for preparation of  $R_2Mo_2O_7$  was as follows: Powders of  $R_2O_3$  and  $MoO_2$  were mixed in appropriate amounts and then pressed into pellets. The pellets were heated in an alumina crucible at about 1400°C in CO/CO<sub>2</sub> gas. The ac susceptibility was measured by the mutual inductance method. The susceptometer consisted of a primary coil of 1200 turns of gauge 40 copper wire. On top of the primary coil we had a secondary coil that consisted of a central segment and two end segments with astatic winding. The secondary coil was balanced and a background signal without the sample was measured from 4.2 to 300 K in a liquid helium cryostat using an oscillator at 80 Hz and an alternating field of approximately 1 G. The signal from the secondary coil was detected using a two-channel lock-in amplifier and the data were collected by an IBM-compatible computer. The sample was placed in the central section of the secondary coil and the signal at this stage was subtracted from the background to give the signal due to the sample. A calibrated Si diode thermometer (Lake shore) was used to measure the temperature of the sample. A

SQUID magnetometer (supplied by Quantum Design, San Diego, CA) was used to measure susceptibility and magnetization.

Electrical resistivity was measured by the usual four-terminal method using a constant current source and a Model 181 Keithley nanovoltmeter. A constant current of 10 mA was used and current direction was reversed to eliminate the thermoelectric effect. The temperature of the sample was measured using a calibrated carbon-glass thermometer (Lake Shore).

## 3. Results and Discussion

### 3.1. AC Susceptibility and Low Field Magnetization

The low field ac susceptibility as a function of temperature is presented in Figs. 2, 3, 4, 5a, and 5b for  $Nd_2Mo_2O_7$ ,  $Sm_2Mo_2O_7$ ,  $Gd_2Mo_2O_7$ ,  $Tb_2Mo_2O_7$ , and  $Y_2Mo_2O_7$ , respectively. Well defined ferromagnetic transition temperatures are observed as sharp peaks in the ac susceptibility at  $T_c = 96, 80,$  and  $57$  K for  $Nd_2Mo_2O_7$  (Fig. 2),  $Sm_2Mo_2O_7$  (Fig. 3), and  $Gd_2Mo_2O_7$  (Fig. 4), respectively. A clear phase transition at 28 K for  $Tb_2Mo_2O_7$  (Fig. 5a) is observed in the ac susceptibility for the first time. This transition appears to be weakly antiferromagnetic or the spin-glass type. A small peak in the ac susceptibility of  $Y_2Mo_2O_7$  (Fig. 5b curve B) is observed at  $\sim 18$  K which corresponds to the spin-glass transition observed by Greedan *et al.* (6).

The low field magnetization measurements as a function of temperature show some very interesting features. Figure 6 shows the  $M$  vs  $T$  data at 50 and 500 G in zero field cooled and field cooled samples of  $Nd_2Mo_2O_7$ . A ferromagnetic transition is observed at  $\sim 96$  K. At low temperature the 50-G curve shows a large hysteresis in the magnetization between the zero field cooled and field cooled curves. Below 20 K there is a large drop in the magnetization.

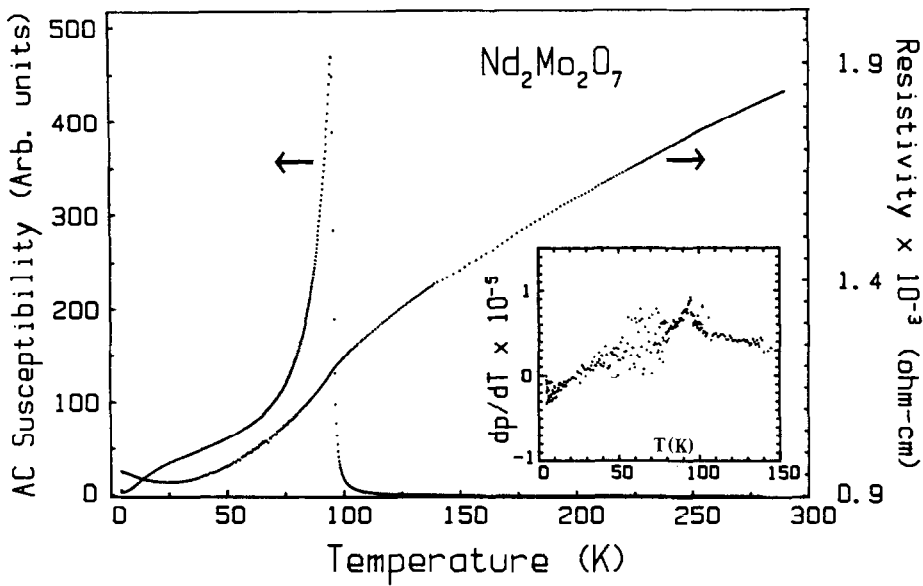


FIG. 2. Electrical resistivity ( $\rho$ ) and ac susceptibility of  $\text{Nd}_2\text{Mo}_2\text{O}_7$  as a function of temperature ( $T$ ). The inset shows the temperature derivative of resistivity ( $d\rho/dT$ ) as a function of temperature in the vicinity of the ferromagnetic transition temperature.

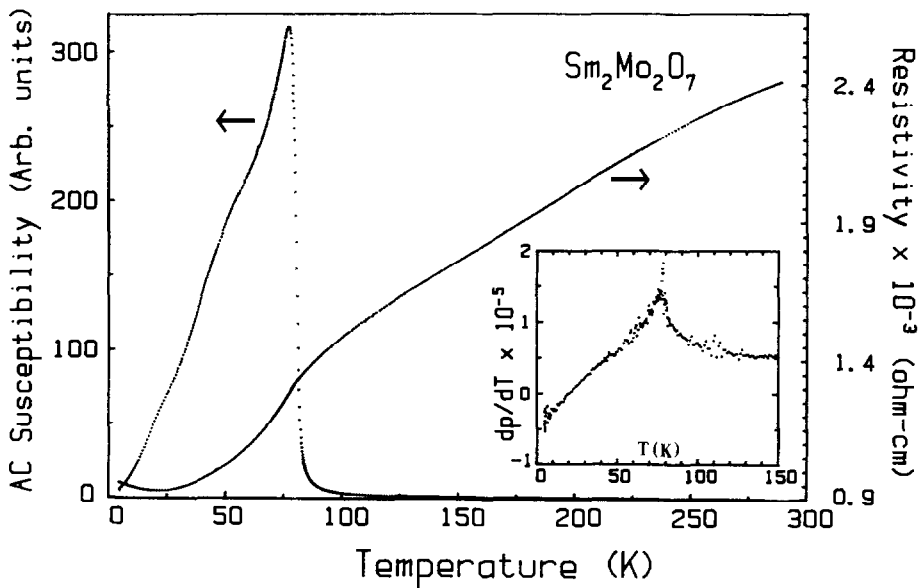


FIG. 3. Electrical resistivity ( $\rho$ ) and ac susceptibility of  $\text{Sm}_2\text{Mo}_2\text{O}_7$  as a function of temperature ( $T$ ). The inset shows the temperature derivative of resistivity ( $d\rho/dT$ ) as a function of temperature in the vicinity of the ferromagnetic transition temperature.

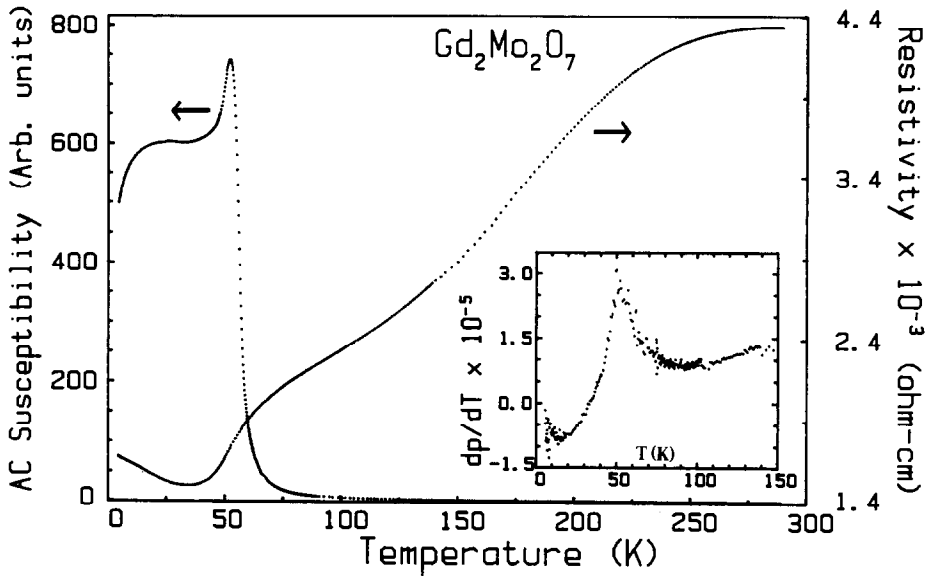


FIG. 4. Electrical resistivity ( $\rho$ ) and ac susceptibility of  $\text{Gd}_2\text{Mo}_2\text{O}_7$  as a function of temperature ( $T$ ). The inset shows the temperature derivative of resistivity ( $d\rho/dT$ ) as a function of temperature in the vicinity of the ferromagnetic transition temperature.

At higher fields (500 G) the hysteresis disappears, but we still observe a drop in the magnetization below 20 K. Figure 7 shows the  $M$  vs  $T$  data for  $\text{Sm}_2\text{Mo}_2\text{O}_7$  at 100 G and 1 kG. Here, too, we observe a ferromagnetic transition at  $\sim 80$  K, a hysteresis in zero field cooled and field cooled magnetization at 100 G, a drop in the magnetization below 25 K, and the disappearance of the hysteresis at high field magnetization. An interpretation of the behavior of  $M$  vs  $T$  data of  $\text{Nd}_2\text{Mo}_2\text{O}_7$  and  $\text{Sm}_2\text{Mo}_2\text{O}_7$  can be put forward as the following. A spontaneous magnetization at  $T_c$  is primarily due to ferromagnetic ordering on the Mo (IV) sublattice. At lower temperature the molecular field from the Mo (IV) sublattice induces a magnetization in the R (III) sublattice. The coupling between Mo (IV)–R (III) appears to be antiferromagnetic, leading to a decrease in the magnetization at low temperatures. Whether this coupling leads to a long range ordered ferrimagnetic state is not

clear. Neutron diffraction data are needed here.

The  $M$  vs  $T$  data for  $\text{Gd}_2\text{Mo}_2\text{O}_7$  at 50 G, 500 G, and 1 kG are presented in Fig. 8. We observe a ferromagnetic transition at  $\sim 56$  K. At low temperatures we do not observe any drop in  $M$  and the magnetization remains constant for 50 G. In the case of  $\text{Gd}_2\text{Mo}_2\text{O}_7$  it appears from the data that both sublattices, the Gd (III) and the Mo (IV), order ferromagnetically simultaneously below  $T_c$  and the coupling between Gd–Mo is ferromagnetic. This interpretation is further supported by the saturation magnetization data on  $\text{Gd}_2\text{Mo}_2\text{O}_7$  discussed in Section 3.2

The low field  $M$  vs  $T$  data for  $\text{Tb}_2\text{Mo}_2\text{O}_7$  at 100 G are presented in Fig. 9. A knee is observed at 25 K as in case of ac susceptibility data. Below 25 K the magnetization increases with decreasing temperature. The knee in the  $M$  vs  $T$  curve at 25 K may be due to a weak antiferromagnetic or spin-glass transition and at lower temperatures

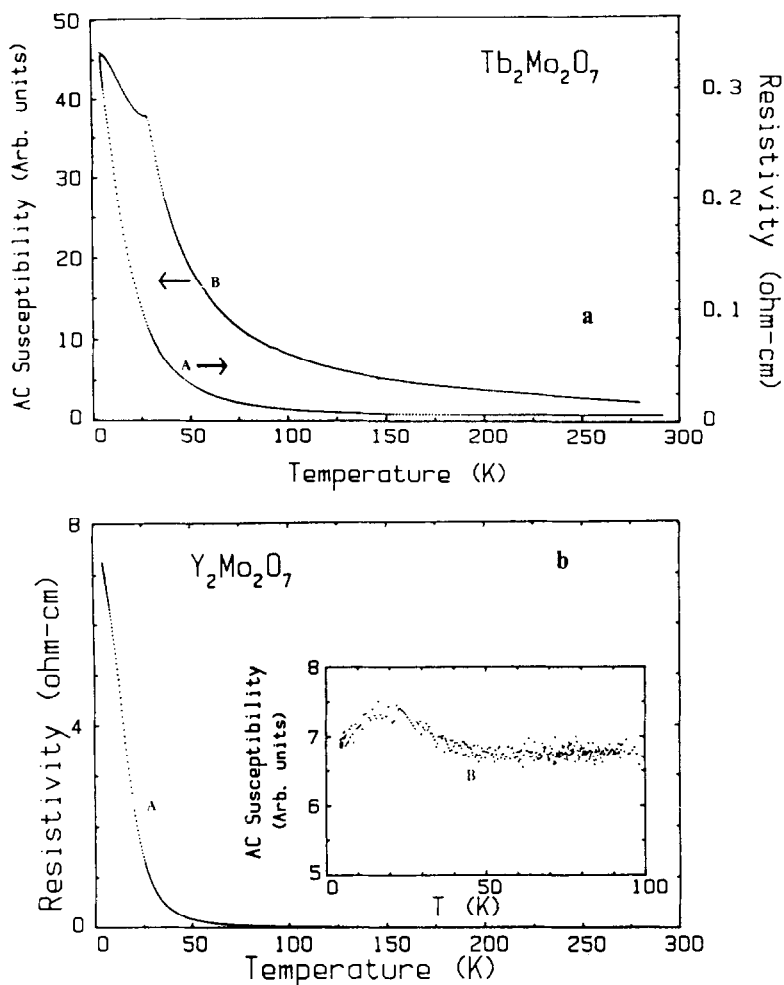


FIG. 5. (a) Electrical resistivity (curve A) and ac susceptibility (curve B) of  $\text{Tb}_2\text{Mo}_2\text{O}_7$  as a function of temperature ( $T$ ) and (b) electrical resistivity (curve A) and ac susceptibility (curve B) of  $\text{Y}_2\text{Mo}_2\text{O}_7$  as a function of temperature ( $T$ ).

the increase in magnetization with decreasing  $T$  is possibly due to the paramagnetic Tb(III) ions.

### 3.2. High Field Magnetization

Isothermal magnetization versus applied field measurements were carried out to fields of 5.5 T compared to 1.5 T in previous studies (4) and the results are shown in Figs. 10a, b, and c. The curves for  $\text{Nd}_2\text{Mo}_2\text{O}_7$  tend to saturate in the temperature range 30 to 80 K with saturation moments

between 2.0 and 2.5  $\mu_B/\text{fu}$ , in agreement with previous work (4) at lower fields. In the temperature range 30 to 80 K the sample magnetization is mostly due to the Mo (IV) sublattice which orders ferromagnetically. The Mo (IV) magnetic moment from the saturation magnetization is estimated to be 1.1  $\mu_B$  per Mo (IV). In the case of  $\text{Nd}_2\text{Mo}_2\text{O}_7$ , the ferromagnetic ordering at  $T_c = 96$  K appears to be due to the Mo (IV) sublattice. At low temperatures (below 30 K) the magnetization curves show an almost

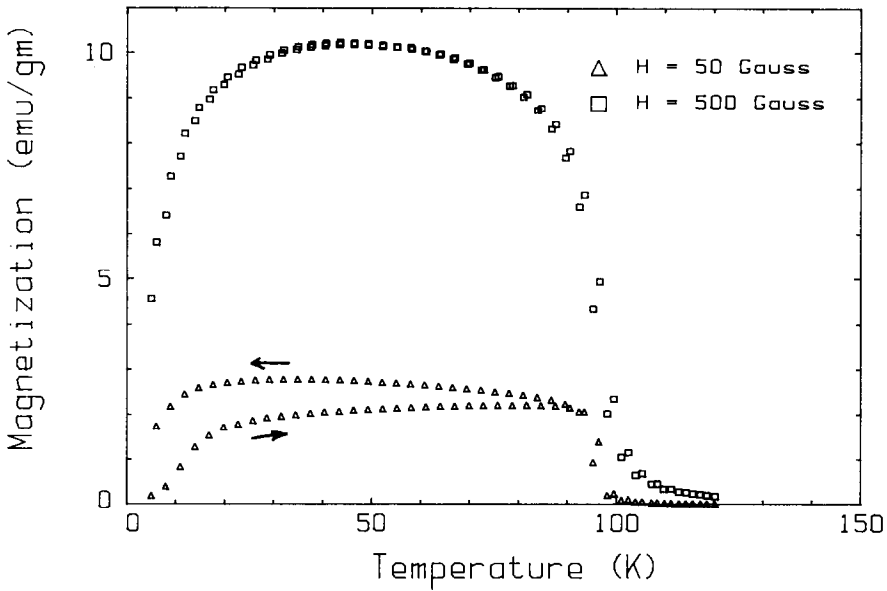


FIG. 6. Magnetization versus temperature for  $\text{Nd}_2\text{Mo}_2\text{O}_7$ .

linear increase in  $M$  vs  $H$  above 5 kG, suggesting an antiferromagnetic coupling between Nd–Mo (IV). Hence, as the temperature is decreased, the sample goes from

paramagnetic to ferromagnetic and then to a possibly ferrimagnetic state.

The magnetization of  $\text{Sm}_2\text{Mo}_2\text{O}_7$  at 5 and 50 K is shown in Fig. 10b. The saturation

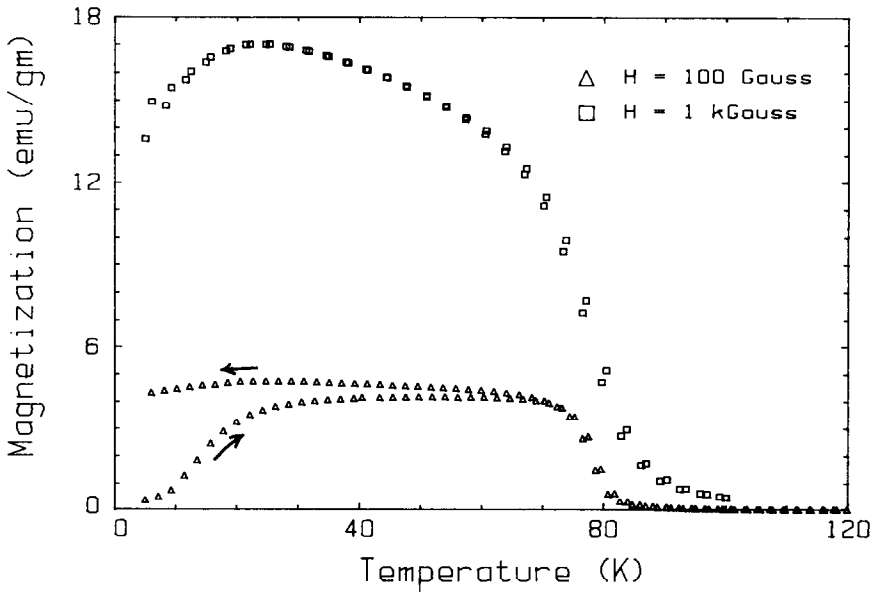


FIG. 7. Magnetization versus temperature for  $\text{Sm}_2\text{Mo}_2\text{O}_7$ .

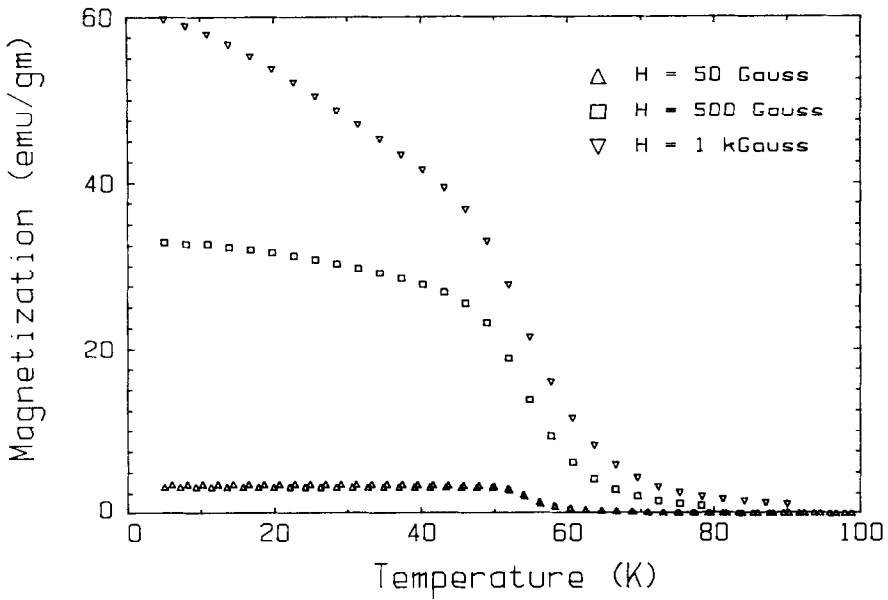


FIG. 8. Magnetization versus temperature for  $\text{Gd}_2\text{Mo}_2\text{O}_7$ .

magnetizations at 5 and 50 K are  $2.7$  and  $2.4 \mu_B/\text{fu}$ , respectively. At low temperature the  $M$  vs  $H$  curve has no large linear contribution in  $\text{Sm}_2\text{Mo}_2\text{O}_7$  as that observed for  $\text{Nd}_2$

$\text{Mo}_2\text{O}_7$ . The ferromagnetic transition at  $T_c = 80$  K in  $\text{Sm}_2\text{Mo}_2\text{O}_7$  appears to be due to the Mo (IV) sublattice as in case of  $\text{Nd}_2\text{Mo}_2\text{O}_7$ . Therefore, the  $M_s = 2.4 \mu_B/\text{fu}$  at 50

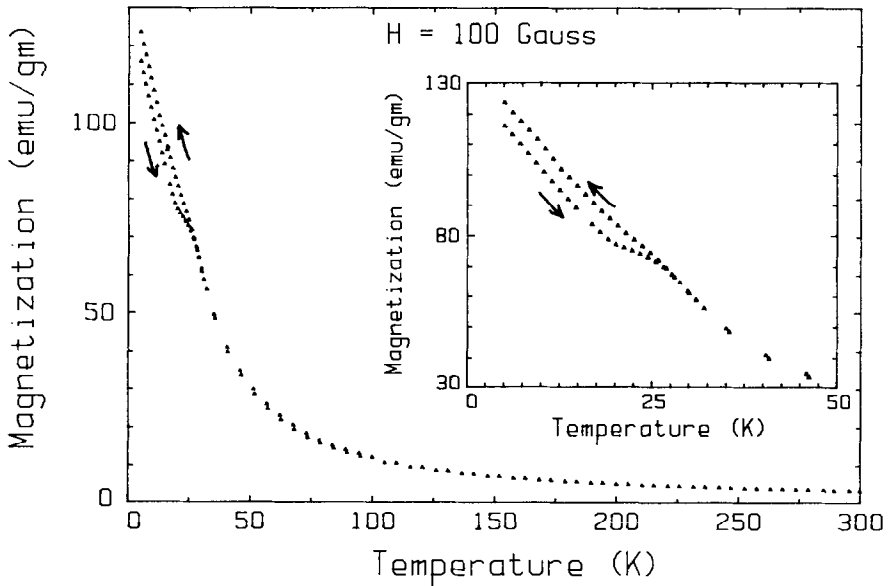


FIG. 9. Magnetization versus temperature for  $\text{Tb}_2\text{Mo}_2\text{O}_7$ . The inset shows the  $M$  vs  $T$  on an enlarged scale.



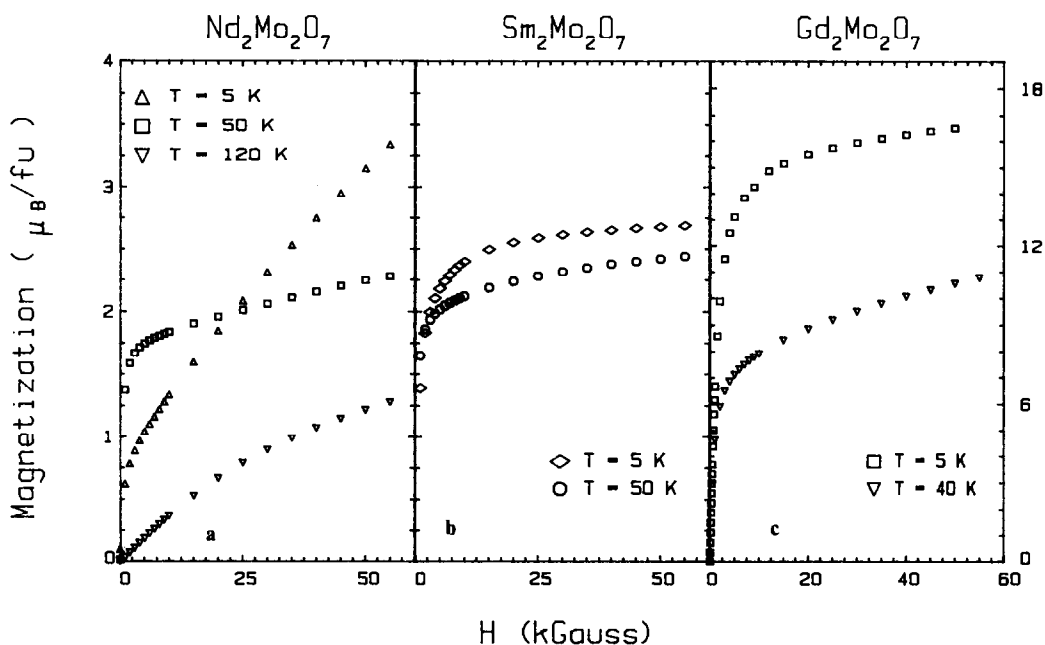


FIG. 10. (a) Magnetization versus applied magnetic field ( $H$ ) for  $\text{Nd}_2\text{Mo}_2\text{O}_7$ , (b) magnetization versus applied magnetic field ( $H$ ) for  $\text{Sm}_2\text{Mo}_2\text{O}_7$ , and (c) magnetization versus magnetic field ( $H$ ) for  $\text{Gd}_2\text{Mo}_2\text{O}_7$ .

K is expected to be largely due to Mo (IV) moments. The saturation moment of Mo (IV) is estimated to be  $1.2 \mu_B$  per Mo (IV), almost the same value as that in  $\text{Nd}_2\text{Mo}_2\text{O}_7$ . At low temperatures an antiferromagnetic coupling between Sm and Mo grows and, possibly, a ferrimagnetic state appears, seen as a decrease in magnetization versus temperature below 25 K (Fig. 7).

The magnetization of  $\text{Gd}_2\text{Mo}_2\text{O}_7$  at 5 and 40 K is presented in Fig. 10c. The saturation magnetization at 5 K is found to be  $16.5 \mu_B/\text{fu}$ . This value is greater than the theoretical value of  $14 \mu_B$  for Gd (III), suggesting a ferromagnetic Mo (IV)–Gd (III) coupling. We estimate the Mo (IV) moment to be  $1.25 \mu_B$  per Mo (IV) in  $\text{Gd}_2\text{Mo}_2\text{O}_7$ . This value of  $1.25 \mu_B$  per Mo (IV) in  $\text{Gd}_2\text{Mo}_2\text{O}_7$  is almost the same as those found for  $\text{Nd}_2\text{Mo}_2\text{O}_7$  and  $\text{Sm}_2\text{Mo}_2\text{O}_7$ . However, the difference is that in case of  $\text{Gd}_2\text{Mo}_2\text{O}_7$  the ferromagnetic transition at  $T_c = 57 \text{ K}$  is most

likely due to both Mo (IV) and Gd (III) sublattices, while in the case of  $\text{Nd}_2\text{Mo}_2\text{O}_7$  and  $\text{Sm}_2\text{Mo}_2\text{O}_7$  the ferromagnetic transitions are primarily due to Mo (IV) sublattice. This is further strengthened by the  $M$  vs  $T$  data (at 50 G) of  $\text{Gd}_2\text{Mo}_2\text{O}_7$  where we observe a constant value of  $M$  below  $T_c$  (Fig. 8).

### 3.3. Resistivity

The resistivity data of Figs. 2, 3, and 4 are essentially identical with those of previous work (5), indicating that the samples have not changed. Analysis of the data in terms of  $d\rho/dT$  vs  $T$  gives peaks which correspond well to the transition temperatures determined by ac susceptibility. The only major difference with previous work is the absence of the high temperature peak in  $d\rho/dT$  at  $\sim 80 \text{ K}$  reported for  $\text{Gd}_2\text{Mo}_2\text{O}_7$ . The lack of any peak in the ac susceptibility at this temperature suggests that the 80 K feature is an experimental artifact.

#### 4. Summary

The onset of long range ferromagnetic order in  $\text{Nd}_2\text{Mo}_2\text{O}_7$ ,  $\text{Sm}_2\text{Mo}_2\text{O}_7$ , and  $\text{Gd}_2\text{Mo}_2\text{O}_7$  was investigated by ac susceptibility methods and Curie temperatures of 96, 80, and 56 K were found, respectively. These correlate well with values obtained from analysis of resistivity data and show that an earlier, higher value for the  $\text{Gd}_2\text{Mo}_2\text{O}_7$  compound was an experimental artifact. Also, a magnetic anomaly at 25 K is reported for  $\text{Tb}_2\text{Mo}_2\text{O}_7$  for the first time. The nature of this low temperature state for  $\text{Tb}_2\text{Mo}_2\text{O}_7$  is probably of the antiferromagnetic or spin-glass type. A spin-glass like transition at about 20 K for  $\text{Y}_2\text{Mo}_2\text{O}_7$ , reported previously, is confirmed by ac susceptibility data.

In a similar temperature range, 20 to 30 K, the magnetization data of  $\text{Nd}_2\text{Mo}_2\text{O}_7$  and  $\text{Sm}_2\text{Mo}_2\text{O}_7$  show significant hysteresis effects, suggesting also a complex magnetic ordering due to antiferromagnetic  $R(\text{III})$ - $\text{Mo}(\text{IV})$  interactions. These materials are

currently under investigation using neutron diffraction methods.

#### Acknowledgments

The work at SIUC was supported by a grant from MTC and ORDA-SIUC and that at McMaster by NSERC.

#### References

1. M. A. SUBRAMANIAN, G. ARAVAMUDAN, AND G. V. SUBBA RAO, *Prog. Solid State Chem.* **15**, 55 (1983), and references therein.
2. M. A. SUBRAMANIAN, G. ARAVAMUDAN, AND G. V. SUBBA RAO, *Mat. Res. Bull.* **15**, 1401 (1980).
3. R. RANGANATHAN, G. RANGARAJAN, R. SRINAVASAN, M. A. SUBRAMANIAN, AND G. V. SUBBA RAO, *J. Low Temp. Phys.* **52**, 481 (1983).
4. M. SATO, XU YAN, AND J. E. GREEDAN, *Z. Anorg. Allg. Chem.* **540/541**, 177 (1986).
5. J. E. GREEDAN, M. SATO, NAUSHAD ALI, AND W. R. DATARS, *J. Solid State Chem.* **68**, 300 (1987).
6. J. E. GREEDAN, N. SATO, XU YAN, AND F. S. RAZAVI, *Solid State Commun.* **59**, 895 (1986).
7. J. N. REIMERS, J. E. GREEDAN, AND M. SATO, *J. Solid State Chem.* **72**, 390 (1987).
8. R. D. SHANNON, *Acta Crystallogr.* **132**, 751 (1976).